DOI:10.1021/jf102514r

JOURNAL OF AGRICULTURAL AND FOOD CHEMISTRY
ARTICLE

Chemical Structures of Corn Stover and Its Residue after Dilute Acid Prehydrolysis and Enzymatic Hydrolysis: Insight into Factors Limiting Enzymatic Hydrolysis

J.-D. Mao,*,† K. M. Holtman,‡ and D. Franqui-Villanueva‡

†Department of Chemistry and Biochemistry, Old Dominion University, 4541 Hampton Blvd, Norfolk, Virginia 23529, United States, and ‡Western Regional Research Center, Agricultural Research Service, U.S. Department of Agriculture, Albany, California 94710, United States

Advanced solid-state NMR techniques and wet chemical analyses were applied to investigate untreated corn stover (UCS) and its residues after dilute acid prehydrolysis (DAP) and enzymatic hydrolysis (RES) to provide evidence for the limitations to the effectiveness of enzyme hydrolysis. Advanced solid-state NMR spectral-editing techniques as well as $^{1}H-^{13}C$ two-dimensional heteronuclear correlation NMR (2D HETCOR) were employed. Our results indicated that dilute acid prehydrolysis selectively removed amorphous carbohydrates, increased aromatic CH/other protonated -C=C- and enriched alkyl CH and CH_2 components. Cinnamic acids were increased, and proteinaceous materials and N-containing degradation or condensation compounds were absorbed or coprecipitated in RES. 2D HETCOR experiments indicated a close association between lignin and the residual carbohydrates. Ketones/aldehydes were not detected in the DAP, in contrast to a report in which an appreciable amount of ketones/aldehydes was generated from the acid pretreatment of a purified cellulose in the literature. This suggested that acid pretreatment may modify the structure of purified cellulose more than biomass and that biomass may be a better substrate than model biopolymers and compounds for assessing structural changes that occur with industrial processing. On the basis of NMR and wet chemical analyses, we found the following factors could cause the limitations to the effectiveness of enzymatic hydrolysis: (1) chemical modification of carbohydrates limited the biologically degradable carbohydrates available; (2) cinnamic acids in the residue accumulated; (3) accessibility was potentially limited due to the close association of carbohydrates with lignin; and (4) proteinaceous materials and N-containing degradation or condensation compounds were absorbed or coprecipitated.

KEYWORDS: Corn stover; NMR; bioethanol; biomass; lignin; cellulose

INTRODUCTION

It is well-known that cellulose in plant materials such as corn stover is encrusted with hemicellulose and lignin in the cell wall. Cellulose conversion is directly related to the removal of hemicellulose and lignin, creating a topochemical effect which opens pore space in the cell wall structure and allows for enhanced accessibility to the cellulose (*1*−*5*). One of the predominating technologies proposed for conversion of this biomass is acid prehydrolysis which has been extensively evaluated by the National Renewable Energy Laboratory (NREL) (*6*−*8*). Acid prehydrolysis solubilizes a significant portion of hemicellulose and some lignin, lowers the degree of polymerization of the cellulose through endwise hydrolysis and random chain scission, creates new reducing end units, and renders the cellulose easily accessible to enzymatic attack.

It has been widely reported that the extent of glucose yield is limited to 70% by dilute acid hydrolysis techniques (*9*−*12*), although Torget et al. (*13*) have reported that an 85% conversion with a shrinking bed percolation reactor was possible. The chemical factors that limit this yield could include glucose degradation (*14*), glucose reversion reactions (*9*), cellulose degradation via parallel parasitic pathways (*15*), modification of cellulose polymers or oligomers (*10*, *11*, *15*, *16*), and repolymerization reactions with lignin intermediates and carbohydrate byproduct (*17*, *18*). Such studies typically utilize monomers or low-molecular-weight materials which are readily solubilized and hence more easily analyzed.

However, in order to enhance the production of ethanol, it is necessary to understand the underlying reasons for the limitations to hydrolysis more clearly by directly studying the insoluble residues after pretreatment and enzymatic hydrolysis. Solid-state NMR spectroscopy is considered as the best choice for the analysis of chemical structures of insoluble organic materials since it is nondestructive and can provide comprehensive structural information. In the past years, we have developed, modified, and adopted many advanced solid-state NMR techniques for the detailed, systematic characterization of complex organic matter (*19*−*21*). Routine ^{13}C solid-state NMR spectra consist of broad and heavily overlapped bands in which functional groups cannot be clearly distinguished.

*To whom correspondence should be addressed. Phone: 757-683-6874. Fax: 757-683-4628. E-mail: jmao@odu.edu.

 Published on Web 10/25/2010

In contrast, our advanced solid-state NMR techniques can selectively retain certain peaks and eliminate others, clearly revealing specific functional groups and allowing for insights into the detailed chemical changes induced by processing. Furthermore, we use $^{1}H-^{13}C$ two-dimensional heteronuclear correlation NMR (2D HETCOR) to detect connectivities or proximities of different functional groups. These advanced NMR techniques are well suited for the detailed characterization of corn stover and its residues after dilute acid pretreatment and enzymatic hydrolysis.

In the present study, we investigated corn stover and its residues after dilute acid prehydrolysis and enzymatic hydrolysis using advanced solid-state NMR spectroscopy as well as wet chemical analysis. The major objectives were (1) to determine the detailed chemical structures of corn stover and its residues and (2) to identify the chemical structures in the residues that may be potentially responsible for limiting the effectiveness of enzymatic hydrolysis.

MATERIALS AND METHODS

Materials. All chemicals were purchased from Fisher Scientific and Sigma-Aldrich and used as received. Corn stover materials were obtained from Novozymes, kindly provided by Dr. Elena Vlasenko, and are representative of the progression of dilute acid prehydrolysis and enzymatic degradation. The acid-pretreated corn stover and the residues after enzymatic hydrolysis were both produced using NREL methods (*6*, *22*). Experimental conditions for dilute acid pretreatment of the corn stover included residence temperature 160 °C, residence time 20 min, and a 0.5% sulfuric acid addition. Enzymatic hydrolysis was conducted under typical conditions. Solids were diluted with pH 4.5 citrate buffer to achieve 5% concentration, and 15 FPU/g cellulase was used. Cellobiase was also added at a 4:1 ratio to the cellulase to avoid feedback inhibition by cellobiose. The flasks were then incubated at 55 °C for 72 h (*23*). After enzymatic incubation, the corn stover residues were washed to maximize glucose removal, and the supernatant was separated via centrifugation. The residues were then lyophilized to ensure biological stabilization. Three samples, untreated corn stover (UCS), residue after dilute acid prehydrolysis (DAP), and residue after enzymatic hydrolysis (RES), were used in the present study.

Methods for Analysis of Cell Wall Components. Acid soluble and insoluble lignin analyses were performed by the standard techniques (*24*). Ash content was performed according to the Technical Association of the Pulp and Paper Industry (TAPPI) test method T-211 om-93. Total monosaccharides were analyzed using the NREL method (*25*). Uronic acids were determined according to Blumenkrantz and Asboe-Hansen (*26*). Cinnamic acid contents were measured by gas chromatography (GC), as described by Ralph et al. (*27*) Elemental analysis was performed by Schwarzkopf Microanalytical Laboratory (Woodside, NY). Protein content was estimated by multiplying the % N from elemental analysis by 6.25 (*28*).

NMR Spectroscopy. All the experiments were performed in a Bruker Avance spectrometer at 75 MHz for ^{13}C, with 4-mm rotors in a double-resonance probe.

^{13}C CP/TOSS and ^{13}C CP/TOSS Plus Dipolar Dephasing. ^{13}C cross-polarization/total sideband suppression (CP/TOSS) experiments with a CP time of 1 ms, a ^{1}H 90° pulse-length of 4 μs, and at a spinning speed of 5 kHz were run to obtain qualitative composition information. ^{13}C CP/TOSS combined with 40-μs dipolar dephasing was employed to generate a subspectrum with signals of nonprotonated carbons and mobile groups such as CH_3. The recycle delay was 3 s.

^{13}C Chemical-Shift-Anisotropy Filter. A five-pulse ^{13}C chemical-shift-anisotropy (CSA) filter (CP-t_{CSA}-180°-pulse-t_{CSA}-90°-pulse-t_z-90°-pulse) (*29*) was inserted into ^{13}C CP/TOSS in order to separate sp^3-hybridized anomeric carbons (O−C−O) from sp^2-hybridized aromatic carbons between 90 and 120 ppm. The ^{1}H 90° pulse-length was 4 μs, contact time 1 ms, and CSA-filter time 47 μs. Four-pulse total suppression of sidebands (TOSS) (*30*) was employed before detection, and two-pulse phase-modulated (TPPM) decoupling was applied for optimum resolution. The CSA filter scheme is combined with an incrementation of the z-period in four steps of $t_r/4$, which provides a "γ-integral" that suppresses sidebands up to the fourth order (*31*). In order to detect nonprotonated anomeric carbons, this filter was combined with a dipolar dephasing time of 40 μs. In contrast, it was also combined with a short CP of 50 μs to obtain selective spectra of protonated anomerics. The recycle delay was 3 s and the spinning speed 5 kHz. The details of this technique are described elsewhere (*29*).

Spectral Editing of Immobile CH_2 + CH. The combined spectrum of these chemical groups was obtained with good sensitivity in a simple spectral-editing experiment. First, a ^{13}C CP/TOSS spectrum is recorded using a short CP of 50 μs. It shows predominantly protonated carbons in immobile segments, but residual peaks of quaternary carbons result from two-bond magnetization transfer. Second, a ^{13}C CP/TOSS spectrum is recorded using a short CP of 50 and 40 μs dipolar dephasing. It contains only the residual signals of quaternary carbons or mobile segments (including CH_3 groups with > 50% efficiency). The difference of the two spectra is the spectrum of immobile CH_2 and CH carbons, with a small CH_3 contribution.

$^{1}H-^{13}C$ Two-Dimensional Heteronuclear Correlation NMR (2D HETCOR NMR). $^{1}H-^{13}C$ heteronuclear correlation (HETCOR) experiments, correlating ^{1}H and ^{13}C chemical shifts in 2D spectra, were also performed. These spectra tell us about the protons in the immediate or wider environment of a given carbon. In particular, the environments of COO/N−C═O groups can be identified, and we can determine whether aromatic, carbohydrate, and alkyl components are in close proximity or not. Especially, in the present study we can use this technique to determine whether the residual cellulose is closely associated with other complex chemical structures, thus limiting further enzymatic hydrolysis. A Lee−Goldburg cross-polarization (LG-CP) of 0.5-ms duration was used so that the correlations between protons and carbons separated by primarily one or two bonds can be detected. We used 128 t_1 increments of 5 μs. In addition, 40 μs dipolar dephasing was inserted in the LG-CP HETCOR to reveal multibond C−H connectivities for nonprotonated carbons. The spinning speed was 6.5 kHz. A detailed description of this technique can be found elsewhere (*32*−*34*).

Table 1. Bulk Properties of Materials Analyzed[a]

	cellulose (%)	lignin (%)	other sugars (%)	ash (%)	protein (%)	uronic acids (%)	total (%)
UCS	36.0	17.2	29.2	4.0	7.1	3.6	97.1
DAP	59.2	26.8	4.3	4.2	2.2	0.6	97.3
RES	17.3	58.2	5.5	9.8	7.3	0.6	98.7

[a] Note that the data are on a dry-weight basis.

RESULTS AND DISCUSSION

Wet Chemistry. The overall conversion of cellulose is 88%, following standard analytical procedures, but not necessarily all carbohydrate is converted to glucose. This is not contradictory to the previous reports that the extent of glucose yield is limited to 70% by dilute acid hydrolysis techniques (*9*−*12*). There remains residual cellulose that is recalcitrant to biochemical degradation. Possible reasons for this recalcitrance may be related to (1) changes in the chemical structure of the residual cellulose, (2) limitation of the accessibility of enzyme due to the close association of cellulose with lignin or lignin residues, (3) adsorption of proteinaceous materials, (4) decreasing enzymatic activity of the cellulase, and (5) the accumulation of chemical moieties that prevent further hydrolysis either through inhibition or limited accessibility. Wet chemistry analyses can provide potential evidence for some of these potential reasons.

Bulk Properties. Table 1 lists the bulk properties as determined by wet chemistry techniques for all three samples. Untreated corn stover prior to dilute acid pretreatment has a cellulose content of 36.0% with additional contributions from hemicelluloses/other sugars (29.2%), lignin (17.2%), protein (7.1%), ash (4.0%), and uronic acids (3.6%). The mass closure also includes acetyl groups and nonstructural sugars (*35*) that were not determined in the present study. After acid pretreatment, DAP contains 59.2% cellulose, 4.3% hemicelluloses/other sugars, 26.8% lignin, 2.2%

Table 2. Total % Monosaccharide Composition of the Three Samples[a]

	glucose	xylose	galactose	arabinose	mannose	total
UCS	55.3	32.8	3.8	5.3	2.8	100
DAP	93.3	4.8	0.6	0.9	0.4	100
RES	76.1	18.0	2.2	3.7	0.0	100

[a] Note that data are on the basis of monosaccharide compositions.

Table 3. Ester- and Ether-Linked Cinnamic Acids in the Samples

	ester-linked		ether-linked		total
	% *p*-coumaric acid	% ferulic acid	% *p*-coumaric acid	% ferulic acid	%
UCS	1.59	0.58	0.71	0.38	3.26
DAP	2.04	0.25	0.15	0.36	2.80
RES	5.00	0.54	0.50	0.94	6.98

protein, 4.2% ash, and 0.6% uronic acids, whereas RES has 17.3% cellulose, 5.5% hemicelluloses/other sugars, 58.2% lignin, 7.3% protein, 9.8% ash, and 0.6% uronic acids. The acid pretreatment concentrates the cellulose in the solid phase to 59.2% of total mass; however, the enzymatic hydrolysis reduces the cellulose content to 17.3%. Lignin is concentrated to 26.8% in DAP and further to 58.2% in RES. The hemicellulose content is significantly reduced in DAP but increase in RES since residual hemicelluloses are not degraded substantially by enzymatic hydrolysis. The protein content is decreased in DAP but increased to 7.3% in RES, indicating the adsorption or coprecipitation of proteins and N-containing degradation/condensation reaction products. Note that protein content estimated by multiplying N content by 6.25 is a fair approximation if we deal with just amino acids; the fact is that amino acids released can give rise to degradation or condensation products. **Table 2** shows that the majority of the remaining hemicellulose constituent is xylose. The hemicellulosic residue is ca. 75% xylose with the remainders being galactose and arabinose in RES. No mannose is detected in RES, indicating a lack of glucomannans and suggesting that the glucose content is entirely cellulosic in nature.

Cinnamic Acids. Cinnamic acids, more specifically *p*-coumaric and ferulic acids, in the cell wall are implicated as the functional groups which connect the carbohydrates and lignin in the cell wall and can be determined by wet chemical techniques (*27*). The incorporation of cinnamic acids into the lignin side chain occurs primarily through esterification or etherification. Esterification occurs at the γ-position on the lignin side chain and may be the nucleation point at which lignification is initiated on the carbohydrate backbone. Etherification occurs primarily through the phenolic hydroxyl on the cinnamic acid moiety, but etherification could also occur at the α-hydroxyl group on the side chain.

In the corn stover materials analyzed here, *p*-coumaric acids are predominant (~70−79% of total) and primarily esterified (**Table 3**). Ferulic acids comprise the remainder and have a higher ratio of ether incorporation (except UCS). Furthermore, the etherified ferulic acid composition appears to be more recalcitrant and accumulates in RES, representing ca. 64% of the total ferulic acid content. The differences in the composition of the two cinnamic acids indicate their different roles in the cell wall. Specifically, *p*-coumaric acid is highly esterified and binds carbohydrates and lignin, whereas the ferulic acid is more highly incorporated into the lignin polymer, thus explaining its higher retention in RES as the etherified structure. The relative recalcitrance of the esterified *p*-coumaric acid may provide evidence of its role in limiting hydrolysis.

The untreated corn stover (UCS) contains 3.26% cinnamic acids on a total weight basis and is reduced to 2.80% by dilute acid prehydrolysis. On a mass balance, the pretreatment is not very effective in removing cinnamic acid moieties even though the esters are acid labile. A harsher treatment would surely provide more complete removal but would also affect the glucose yields. Retention of the cinnamic acids strongly suggests that inhibition of enzyme hydrolysis be at least partially associated with accessibility related to the close association of cellulose with lignin that the cinnamates provide. The total cinnamic acid content is increased to 6.98% in RES, providing the possible evidence of their role in limiting hydrolysis.

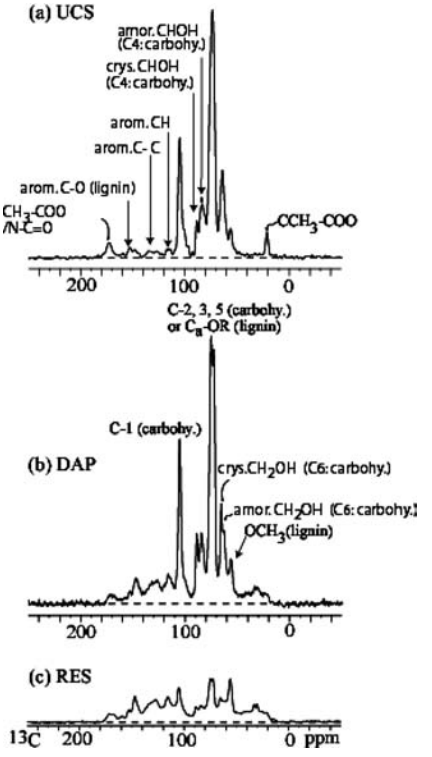

Figure 1. ^{13}C CP/TOSS spectra of (**a**) UCS, (**b**) DAP, and (**c**) RES. Note that with enzymatic hydrolysis, the cellulose (around 60−110 ppm) is significantly reduced.

NMR Spectroscopy. *Semiquantitative CP/TOSS Spectra.* **Figure 1a-c** show semiquantitative ^{13}C CP/TOSS spectra of UCS, its residues after dilute acid pretreatment (DAP), and after enzymatic hydrolysis (RES), respectively. The ^{13}C CP/TOSS spectrum of UCS (**Figure 1a**) is dominated by signals from 60−110 ppm representative of the carbohydrate fraction; other signals are small by comparison. The lignin signals in corn stover can be observed relatively unobstructed by the broad resonances ranging from 110−160 ppm, attributed to the signals of aromatic carbons. The chemical shift of the OCH_3 groups on the lignin aromatic ring resides around 56 ppm. The peak intensity of the lignin is small in comparison to the carbohydrate signals. The lignin in corn stover is a mixture of guaiacyl (G) and syringyl (S), with a small amount of the *p*-hydroxyphenyl (H) lignin. The COO/N−C═O resonances around 165−180 ppm are due to the acetyl side groups on the xylan, glucuronic acids, and cinnamic acids, and N−C═O of peptides and proteins. The methyl groups associated with the acetyl moiety resonate at 22 ppm. The detailed assignments of lignin and carbohydrates in corn stover are listed in **Table 4**.

Compared to the ^{13}C CP/TOSS spectrum of UCS (**Figure 1a**), two general differences exist with that of the stover after dilute acid prehydrolysis (DAP) (**Figure 1b**). First, dilute acid prehydrolysis enhances and broadens ^{13}C NMR signals above 110 ppm and also below 50 ppm, indicating the accumulation of lignin and

Table 4. NMR Chemical Shifts of Cellulose and Lignin Moieties in Corn Stover[a]

moiety	chemical shift (ppm)
aldehyde/ketone (C═O)	180−220
COO acid/ester(COO)	165−180
aromatic C−O (G_3, G_4, $S_{3(e\ and\ ne)}$, and $S_{5(e\ and\ ne)}$)	153−143
aromatic C−C ($G_{1(e)}$, $S_{1(e\ and\ ne)}$, and $S_{4(e\ and\ ne)}$)	134−137
aromatic C−C ($G_{1(ne)}$)	131
aromatic C−H (G_6 of lignin)	120
aromatic CH (G_5 of lignin)	115
aromatic CH (G_2 of lignin)	112
aromatic CH (S_2 and S_6)	106
OCHO of carbohydrates (C_1 of cellulose)	105
CHOH of carbohydrates (crystalline C_4 of cellulose)	89
CHOH of carbohydrates (amorphous C_4 of cellulose)	84
C_β-OR of lignin	86−82
CHOH of carbohydrates (C_2, C_3, C_5, of cellulose)	75
C_α-OR of lignin	76−72
CHOH of carbohydrates (C_2, C_3, C_5, of cellulose)	72
CH_2OH of carbohydrates (crystalline C_6 of cellulose)	66
CH_2OH of carbohydrates (amorphous C_6 of cellulose)	63
C_γ-OR of lignin	64−60
OCH_3 of lignin	56
CH_3 of hemicelluloses (CH_3-COO)	22

[a] Note that e indicates etherified units in C4, and ne refers to nonetherified (phenolic) units in C4 (*43*−*45*). G is the guaiacyl lignin unit, and S is the syringyl lignin unit.

the generation of other functional groups; and second, the carbohydrate signals between 60 and 110 ppm are more resolved for the spectrum of the DAP than for that of the UCS, showing that dilute acid prehydrolysis selectively removes amorphous carbohydrates. The ^{13}C CP/TOSS spectra of the DAP and RES (**Figures 1b** and **c**) are quite similar except for the significant removal of carbohydrate signals between 60 and 110 ppm for RES.

Spectral-Editing Revealing Specific Functional Groups. The detailed characterization of RES can provide the opportunity to elucidate the structure of the remaining cell wall components and explain the limits of hydrolysis after dilute acid prehydrolysis. Therefore, we conducted much more detailed NMR analyses of RES than UCS and DAP; the spectral editing techniques which can identify specific functional groups as well as 2D HETCOR showing the connectivities or proximities of different functional groups were applied for this sample (**Figures 3** and **4**). For comparison, we also include simple spectral-editing spectra of UCS and DAP, including those of dipolar dephasing and the ^{13}C CSA filter (**Figure 2**).

Figure 2 shows ^{13}C CP/TOSS, dipolar-dephased, and ^{13}C CSA-filtered spectra of UCS and DAP. **Figure 3** shows the spectral-editing spectra of RES; in addition to the dipolar-dephased and ^{13}C CSA-filtered spectra (**Figures 3b** and **c**), we also acquired spectra with the ^{13}C CSA-filter, ^{13}C CSA-filter plus short CP, and ^{13}C CSA filter plus dipolar dephasing as well as CH_n-only selection.

The dipolar-dephased spectra (**Figure 2b** and **e** and **Figure 3b**) solely exhibit resonances of nonprotonated carbons and carbons of mobile groups such as the highly mobile CCH_3 at 22 ppm and OCH_3 at 56 ppm. Nonprotonated aromatic carbons (aromatic C−O and aromatic C−C) resonate from 120 to 160 ppm with the aromatic C−O signal around 153 ppm and the aromatic C−C signal around 130 ppm. Also, the N−C═O/COO signal around 173 ppm is present. Furthermore, a mobile−mobile CCH_2C group band is present in the dipolar-dephased spectrum of RES (**Figure 3b**).

The ^{13}C CP/TOSS spectrum after a CSA filter, which exhibits only sp^3-hybridized carbons, is displayed in **Figures 2c** and **f** and **Figure 3c**. This technique separates overlapping anomerics (O−C−O) from aromatics between 90 and 120 ppm and results in an isolated

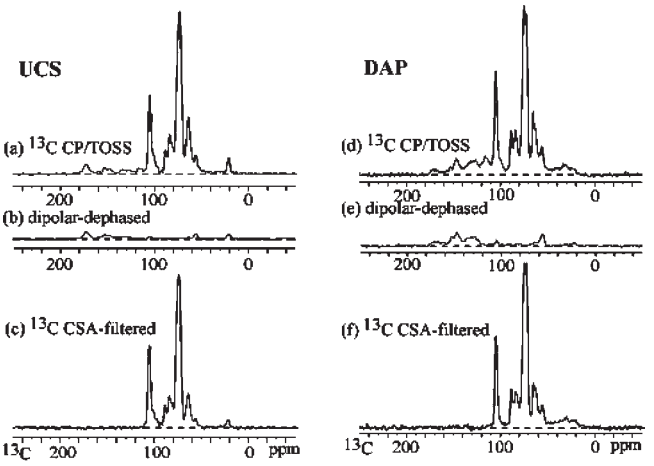

Figure 2. Simple spectral-editing spectra of UCS (**a**−**c**) and DAP (**d**−**f**). (**a** and **d**) ^{13}C CP/TOSS spectra. (**b** and **e**) Dipolar dephased spectra. (**c** and **f**) ^{13}C CSA-filtered spectra.

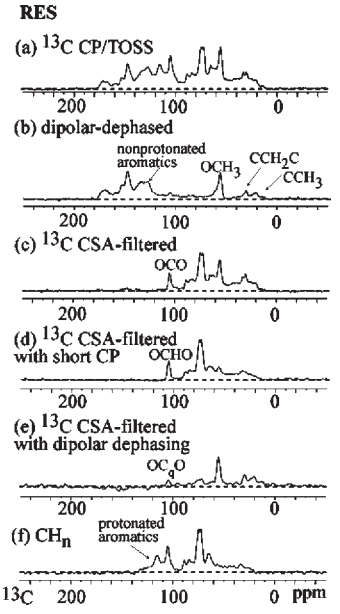

Figure 3. Detailed spectral editing of RES. (**a**) Full ^{13}C CP/TOSS spectrum for reference with a contact time of 1 ms. (**b**) Dipolar-dephased spectrum showing nonprotonated carbons and carbons of mobile segments such as CH_3 and OCH_3 with 40-μs dephasing time. (**c**) Selection of alkyl and O-alkyl carbons with a ^{13}C CSA filter, which in particular identifies OCO carbons typical of sugar rings. CSA filter time: 47 μs. (**d**) Selection of protonated alkyl and O-alkyl carbons with a CSA filter and short CP, in particular OCHO around 105 ppm. CSA filter time 47 μs. CP time 50 μs. (**e**) Selection of nonprotonated and mobile alkyl and O-alkyl carbons with a CSA filter and dipolar dephasing, which in particular identifies OC(RR′)O carbons, with a CSA filter time of 47 μs and dipolar dephasing of 40 μs. (**f**) Selection of immobile CH and CH_2.

O−C−O peak at 105 ppm characteristic of the C_1 of carbohydrates such as those of cellulose and hemicelluloses for all three samples.

For RES, we also have three more spectral-editing spectra. The combination of the CSA filter technique with short CP (50 μs) results in a subspectrum of protonated alkyl and O-alkyl carbons (**Figure 3d**). In particular, a clear band of protonated O-CH-O moieties is visible at 105 ppm. Obviously, most anomerics are protonated. The carbohydrate signals ranging around 60−90 ppm of the reference ^{13}C CP/TOSS spectrum are quite similar to those of **Figure 3d**, indicating that theses carbons are primarily protonated.

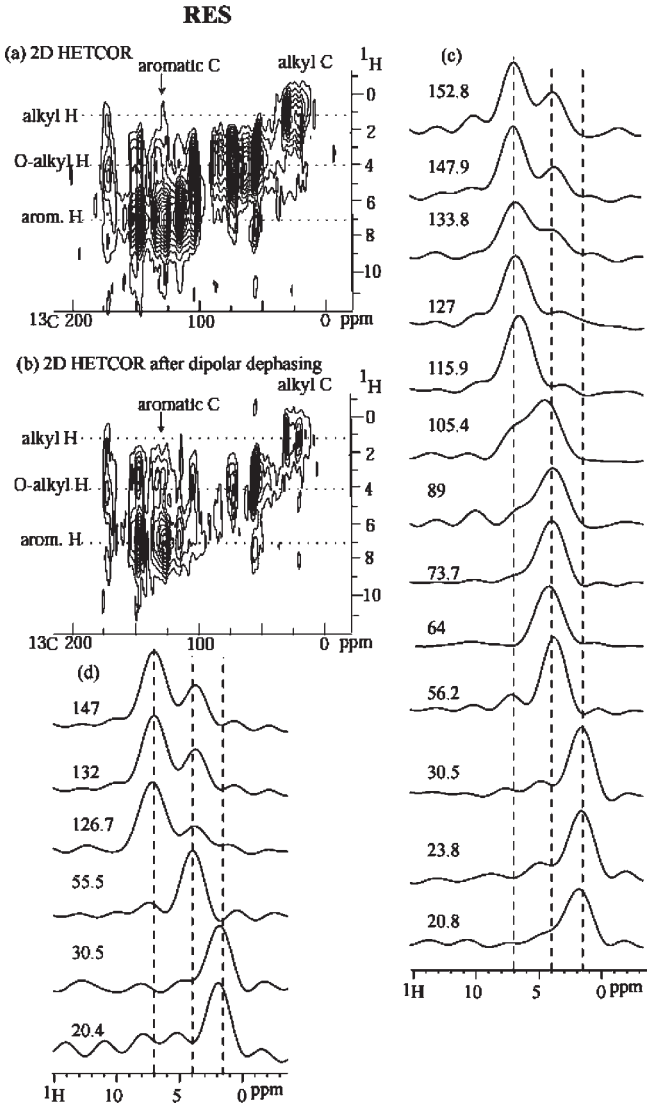

Figure 4. Identification of functional groups in RES by ^{1}H−^{13}C HETCOR without spin diffusion and with 0.5-ms LGCP. (**a**) Contour plot of the two-dimensional spectrum. (**b**) Same as in **a** but with dipolar dephasing. (**c**) Cross-sections from spectrum **a** at the indicated ^{13}C chemical shifts: 20.8, 23.8, 30.5, 56.2, 64, 73.7, 89, 105.4, 115.9, 127, 133.8, 147.9, and 152.8 ppm. (**d**) Cross-sections from spectrum **a** at the indicated ^{13}C chemical shifts: 20.4, 30.5, 55.5, 126.7, 132, and 147 ppm.

Since OCH_3 carbons have the largest ^{13}C chemical shift anisotropies among all the sp^3-hybridized carbons, their signals are much more reduced compared with other O-alkyls. The combination of this filter technique with dipolar dephasing (**Figure 3e**) shows that small amounts of quaternary O-C_q-O groups are present in this sample. **Figure 3f** displays the spectrum with immobile CH plus CH_2 and a small amount of CH_3, attributed to the protonated aromatics (aromatic C−H) around 115 ppm, protonated carbohydrate signals from 60 to 110 ppm, and a broad band from 0 to 60 ppm attributed to OCH_3, CCHC, CCH_2C, and CCH_3.

Structural Information from Short-Range HETCOR. **Figure 4a** displays the ^{1}H−^{13}C HETCOR spectrum of RES with 0.5 ms of LGCP, which primarily but not exclusively shows correlation peaks for one- and two-bond distances. The proton cross-sections at the indicated ^{13}C chemical shifts were extracted to help identify the connectivities or proximities of different functional groups (**Figure 4c**). At the ^{13}C chemical shifts of 152.8 and 147.9 ppm where aromatic C−O groups resonate, the significant contribution is from O-alkyl such as OCH_3 protons; correspondingly, the cross-section at the ^{13}C chemical shift of 56.2 ppm displays a small band at ca. 7 ppm from the aromatic protons. This shows a correlation between OCH_3 and aromatics in lignin functionalities and provides an example of interpreting the HETCOR spectrum. The cross-section at the ^{13}C chemical shift of 133.8 ppm attributed to nonprotonated aromatic carbons shows a significant correlation with the protons of O-alkyls such as those on the lignin aromatic ring or possibly of carbohydrates. The contributions of O-alkyl protons for slices at 127 and 115.9 ppm are not as significant as that for the slice at 133.8 ppm. Correspondingly, the slices representing carbohydrates at 105.4 ppm and 89 ppm show correlation proton slices from the aromatic protons, indicating that aromatics from components such as lignin are closely associated with carbohydrates, in part explaining the limits of hydrolysis. The ^{1}H slices at 73.7 ppm and 64 ppm of carbohydrates primarily correlates with their own protons. Similarly, the ^{1}H slices at 30.5, 23.8, and 20.8 of CCH_2 and CCH_3 show correlations primarily with their own protons, although slight shoulders from the O-alkyl protons can be observed.

The ^{1}H−^{13}C 2D HETCOR spectrum with 40-μs dipolar dephasing shows nontrivial correlation peaks of nonprotonated carbons with the nearest ^{1}H, which are at a distance of at least two bonds (**Figure 4b**). ^{1}H slices were extracted at the ^{13}C chemical shifts of 147, 132, 126.7, 55.5, 30.5, and 20.4 ppm. Aromatic C−O at 147 ppm correlate most prominently with OCH_3 protons (**Figure 4d**), and OCH_3 at 55.5 ppm correlates with aromatic protons, attributed to those of lignin. Aromatic carbons at 132 and 126.7 ppm clearly show some correlation with O-alkyl protons. The methyl groups at 20.4 ppm and mobile CCH_2C groups at 30.5 ppm are primarily associated with their own protons.

Chemical Structural Changes after Dilute Acid Prehydrolysis and Enzymatic Hydrolysis. On the basis of ^{13}C CP/TOSS and spectral-editing spectra, we obtained semiquantitative structural information on the three samples. The CP/TOSS data are corrected based upon simulation and reported as quantitative data in **Table 5** on a percentage basis (*36*, *37*).

On the basis of **Table 5**, we discuss the detailed, quantitative chemical structural changes after dilute acid prehydrolysis and enzymatic hydrolysis, primarily ordered from downshift to upshift according to their ^{13}C NMR resonance positions.

Aldehydes/Ketones (220−180 ppm). In the ^{13}C CP/TOSS spectra shown in **Figure 1**, we do not observe any signals of aldehydes or ketones for all three samples. Qian et al. (*16*)

Table 5. Percentages of Different Functional Groups Obtained by ^{13}C CP/TOSS Combined with Spectral Editing[a]

	assign. (ppm)	UCS	DAP	RES
C=O	220−180	0	0	0
COO/N−C=O	180−165	4.5	0.5	1.1
aromatic C−O	165−142	5.4	8.6	15.9
aromatic C−C/other nonprotonated -C=C-	142−111	2.5	4.7	9.8
aromatic C−H/other protonated -C=C-	135−103	6.1	20	28.7
aromatic/-C=C- total	165−103	14.0	33.3	54.4
acetal	112−95	14.6	9.0	2.7
ketal	112−95	0.5	0.6	1.3
O-alkyl	95−59	57.9	47.2	20.3
OCH_3/NCH	59−50	3.7	4.5	9.5
CH/CH_2	50−24	1.8	4.6	8.0
CH_3	24−0	3.0	0.4	2.8
total	220−0	100	100.1	100.1

[a] ^{13}C CP/TOSS data were corrected on the basis of the protocol described elsewhere (*36*, *37*), and errors due to CP/TOSS correction are ca. 5%. Overlapping functional groups were separated on the basis of spectral-editing techniques.

reported an appreciable amount of ketone/aldehyde structures resulting from acid pretreatment of a purified cellulose standard. Our results are inconsistent with theirs, suggesting that acid pretreatment may modify the structure of a purified cellulose more than a biomass in which the cellulose is encrusted with lignin and hemicelluloses and potentially protected. This result shows the necessity of nondestructive analysis of corn stover residues, rather than of pure model compounds, by solid-state NMR for finding evidence of limited hydrolysis.

COO/N−C═O Groups (*180−165 ppm*). The COO/N−C═O resonances are attributed to the acetyl side groups and N−C═O from peptides and proteins. The amount of COO/N−C═O is reduced after the acid pretreatment and enzymatic hydrolysis (**Table 5**). After dilute acid pretreatment, COO/NCO structures are reduced from 4.5% in UCS, to 0.5% in DAP and to 1.1% in RES.

Aromatic C−O Groups (*165−142 ppm*). After processing, aromatic C−O attributed to lignin is increased (**Table 5**), consistent with higher lignin in DAP and RES based on **Table 1**. Aromatic C−O is 5.4% in UCS (**Table 5**). This translates to 2.36 C per aromatic ring (C/Ar) when considering the whole aromatic contribution (165−100 ppm). The aromatic C−O content is similar to that of a gauaicyl lignin, indicating that the S:G ratio is low.

Aromatic C−C and Other Nonprotonated -C═C- (*142−111 ppm*). The aromatic C−C and other nonprotonated -C═C- content follows a trend of enrichment through pretreatment and enzyme hydrolysis (**Table 5**). The nonprotonated aromatic and -C═C- carbons increase from 2.5% in UCS to 4.7% and 9.8%, respectively, in DAP and RES.

Aromatic C−H and Other Protonated -C═C- (*135−103 ppm*). If all this region is attributed to aromatic C−H, then the aromatic C−H is above the theoretical value for lignin content, suggesting a large accumulation of this functional group from reactions occurring during acid prehydrolysis. Correspondingly, there is a loss of carbons in the O-alkyl (95−59 ppm) in DAP and RES. This shift could be interrelated. The data suggest that acid prehydrolysis could cause those carbons on either the carbohydrate polymer or the lignin side chain to become unsaturated, likely through a dehydration reaction (*15*, *38*−*41*) or, in the case of lignin, the loss of formaldehyde and vinyl ether formation (*42*). Unsaturated -C═C- bonds on carbohydrate backbones may limit enzyme hydrolysis, and it is likely that a considerable portion of the side reactions occur on the cellulose polymer. The aromatic C−H and other protonated -C═C- percentages increase from 6.1% in UCS to 20% and 28.7% in DAP and RES, respectively.

Anomerics (*112−95 ppm*). The ^{13}C CSA filter experiment selects sp^3-hybridized carbons and unobscures overlap specifically between anomeric and aromatic carbons. Protonated acetal and nonprotonated ketal can be separated by the ^{13}C CSA filter combined with short CP or dipolar dephasing. Consistent with the decrease of carbohydrates, anomerics are reduced from 15.1% to 9.6% for UCS and to 4.0% for RES. Ketal accounts for a very small portion of anomerics. On the basis of the ^1H slice of 2D HETCOR spectrum (105.4 ppm of **Figure 4c**), anomerics are closely associated or bonded to aromatics. Anomerics directly bonded to aromatics cannot form double bonds but can still be detected around 100 ppm.

O-Alkyl (*95−59 ppm*). The ^{13}C chemical shifts of the O-alkyl moieties (95−59 ppm) are primarily attributed to C_2−C_6 of carbohydrates and the C_α-OR, C_β-OR, and C_γ-OR on the lignin side chain (**Table 4**). The total carbon amount of O-alkyls in UCS accounts for 57.9% including carbohydrates and lignin. In DAP, the O-alkyls account for 47.2% and are reduced to 20.3% in the RES.

OCH_3 and NCH Structures (*59−50 ppm*). These functional groups for UCS account for 3.7%. In addition to OCH_3 groups, N−CH resonances from protein or peptide structures contribute to this region as do small amounts of lignin aliphatic sidechian carbons. They increase from 3.7% in UCS to 4.5% in DAP and 9.5% in RES, mirroring the increase of the adsorption and coprecipitation of proteins and N-containing degradation or condensation compounds and lignin as determined by elemental analysis.

Alkyl CH and CH_2 (*50−24 ppm*). This region for UCS is primarily associated with alkyl carbons on the lignin side chains from interunit linkages such as dihydroconiferyl alcohol (DHCA) or those associated with protein side chains. Since lipids and wax are not removed, signals of lipids and/or wax may also contribute significantly to this region. They represent 1.8% in UCS and increase to 4.6% for DAP. This indicates that alkyl structures are enriched during dilute acid prehydrolysis, although the mechanism is unclear. RES contains 8.0% for this region.

Methyl (*24−0 ppm*). Methyl groups are highest in UCS (3.0%), related directly to acetyl groups on the glucuronoxylan backbone and also some to side chains of proteins. The acetyl groups are readily hydrolyzed under acidic conditions, and this is corroborated as DAP contains little methyl content (0.4%). The CH_3 content is enriched to 2.8% in RES, which could be partially derived from the absorbed or coprecipitated proteins/peptides.

Potential Factors Limiting Enzymatic Hydrolysis As Determined in the Present Study. Potential reasons for the limitation of enzyme hydrolysis as determined by the present study are (1) the recalcitrant nature of the residual cellulose, in part, due to chemical modification from pretreatment; (2) enrichment of the cinnamic acids as hydrolysis proceeds; (3) limitation of the accessibility of the enzyme due to the close association of the hemicellulose and cellulose with lignin; and (4) adsorption or coprecipitation of proteinaceous materials and N-containing degradation or condensation compounds, decreasing enzymatic activity of the cellulase.

NMR data indicates that the primary structural change occurring with dilute acid prehydrolysis pretreatment is the accumulation of protonated aromatics and -C═C- carbons which could be related to the formation of unsaturated carbons from carbohydrates, likely through dehydration reactions. Other changes observed by NMR include an accumulation of alkyl CH and CH_2 groups, although it is unclear whether these are associated with lignin, carbohydrates, or proteins.

Cinnamic acids play a pivotal role in cross-linking polysaccharides and lignin in the cell wall. In the materials studied here, *p*-coumaric acids predominate, and cinnamic acids are accumulated in RES to 6.98% on a total weight basis.

As expected, small amounts of hemicellulosic residues remain and are mostly retained throughout enzymatic hydrolysis. The hemicellulose or cellulose residues are tightly associated with or bonded with lignin, as confirmed by our 2D HETCOR experiments. RES contains 58.2% lignin by weight, and therefore, it might be inferred that the residual carbohydrate is recalcitrant due to its association with lignin.

Protein content increases with hydrolysis from 2.2% in DAP to 7.3% in RES on a weight basis as determined from wet chemical analysis, indicating adsorption or coprecipitation of proteinaceous materials and N-containing degradation or condensation compounds.

Summary. The present study utilizes wet chemical analysis and solid-state NMR experiments to glean detailed chemical structural information on untreated corn stover and its hydrolysis and enzymatic residues. The advanced solid-state spectral-editing

techniques allow for detailed investigations of structural changes occurring with pretreatment and hydrolysis.

Dilute acid prehydrolysis

- selectively removes amorphous carbohydrates, and the NMR signals of remaining carbohydrates are better resolved.
- accumulates protonated aromatic and -C=C- carbons which could be due to modifications of the structure of residual carbohydrates.
- generates CH and CH_2 alkyl components as detected by solid state NMR.

Potential evidence for limitations of hydrolysis have been detailed. From the solid-state NMR and wet chemistry, it has been determined that the following factors could contribute to limiting hydrolysis in ethanol production, including

- chemical modification of carbohydrates
- accumulation of cinnamic acids in the residues
- potential limitation of accessibility due to the close association of carbohydrates with lignin
- adsorption or coprecipitation of proteinaceous materials and N-containing degradation or condensation compounds.

ABBREVIATIONS USED

UCS, untreated corn stover; DAP, residue after dilute acid prehydrolysis; RES, residue after enzymatic hydrolysis; NREL, National Renewable Energy Laboratory; TAPPI, Technical Association of the Pulp and Paper Industry; GC, gas chromatography; NMR, nuclear magnetic resonance; CP/TOSS, cross-polarization/total sideband suppression; CP, cross-polarization; TOSS, total suppression of sidebands; CP/MAS, cross-polarization/magic angle spinning; TPPM, two-pulse phase-modulated; CSA, chemical-shift-anisotropy; 2D HETCOR, two-dimensional $^{1}H-^{13}C$ heteronuclear correlation nuclear magnetic resonance; LGCP, Lee−Goldburg cross-polarization; G, guaiacyl; S, syringyl; H, *p*-hydroxyphenyl; DHCA, dihydroconiferyl alcohol.

LITERATURE CITED

(1) Fang, X.; Shen, Y.; Zhao, J.; Bao, X. M.; Qu, Y. B. Status and prospect of lignocellulosic bioethanol production in China. *Bioresour. Technol.* **2010**, *101*, 4814−4819.

(2) Kaparaju, P.; Serrano, M.; Thomsen, A. B.; Kongjan, P.; Angelidaki, I. Bioethanol, biohydrogen and biogas production from wheat straw in a biorefinery concept. *Bioresour. Technol.* **2009**, *100*, 2562−2568.

(3) Conte, P.; Maccotta, A.; De Pasquale, C.; Bubici, S.; Alonzo, G. Dissolution mechanism of crystalline cellulose in H3PO4 as assessed by high-field NMR spectroscopy and fast field cycling NMR relaxometry. *J. Agric. Food. Chem.* **2009**, *57*, 8748−8752.

(4) Kerr, A. J.; Goring, D. A. I. The ultrastructural arrangement of the wood cell wall. *Cellul. Chem. Technol.* **1975**, *9*, 563−573.

(5) Matsushita, Y.; Inomata, T.; Hasegawa, T.; Fukushima, K. Solubilization and functionalization of sulfuric acid lignin generated during bioethanol production from woody biomass. *Bioresour. Technol.* **2009**, *100*, 1024−1026.

(6) Aden, A.; Ruth, M.; Ibsen, K.; Jechura, J.; Neeves, K.; Sheehan, J.; Wallace, B.; Montague, L.; Slayton, A.; Lukas, J. Lignocellulosic Biomass to Ethanol Process Design and Economics Utilizing Co-current Dilute Acid Prehydrolysis and Enzymatic Hydrolysis for Corn Stover. *NREL/TP-510-32438*. National Renewable Energy Laboratory: Golden, CO, USA 2002.

(7) Wooley, R.; Ruth, M.; Sheehan, J.; Ibsen, K. Lignocellulosic Biomass to Ethanol Process Design and Economics Utilizing Co-current Dilute Acid Prehydrolysis and Enzymatic Hydrolysis Current and Futuristic Scenarios. *NREL/TP-580-26157*. National Renewable Energy Laboratory: Golden, CO, USA, 1999.

(8) Himmel, M. E.; Ding, S.-Y.; Johnson, D. K.; Adney, W. S.; Nimlos, M. R.; Brady, J. W.; Foust, T. D. Biomass recalcitrance: Engineering plants and enzymes for biofuels production. *Science* **2007**, *315*, 804−807.

(9) Conner, A. H.; Wood, B. F.; Hill, D. G.; Harris, J. F. Kinetic model for the dilute sulfuric acid saccharification of lignocellulose. *J. Wood Chem. Technol.* **1985**, *5*, 461−489.

(10) Abatzoglou, N.; Bouchard, J.; Chornet, E.; Overend, R. P. Dilute acid depolymerization of cellulose in aqueous phase: Experimental evidence of the significant presence of soluble oligomeric intermediates. *Can. J. Chem. Eng.* **1986**, *64*, 781−786.

(11) Bouchard, J.; Abatzoglou, N.; Chornet, E.; Overend, R. P. Characterization of depolymerized cellulosic residues. Part 1: Residues obtained by acid hydrolysis processes. *Wood Sci. Technol.* **1989**, *23*, 343−355.

(12) Bouchard, J.; Overend, R. P.; Chornet, E.; Van Calsteren, M.-R. Mechanism of dilute acid hydrolysis of cellulose accounting for its degradation in the solid state. *J. Wood Chem. Technol.* **1992**, *12*, 335−354.

(13) Torget, R. W.; Kim, J. S.; Lee, Y. Y. Fundamental aspects of dilute acid hydrolysis/fractionation kinetics of hardwood carbohydrates. 1. Cellulose hydrolysis. *Ind. Eng. Chem. Res.* **2000**, *39*, 2817−2825.

(14) Saeman, J. F. Kinetics of wood saccharification. *Ind. Eng. Chem. Res.* **1945**, *37*, 43−52.

(15) Mok, W. S.-L.; Antal, M. J., Jr. Productive and parasitic pathways in dilute acid-catalyzed hydrolysis of cellulose. *Ind. Eng. Chem. Res.* **1992**, *31*, 94−100.

(16) Qian, X.; Nimlos, M. R.; Davis, M.; Johnson, D. K.; Himmel, M. E. Ab initio molecular dynamics simulations of β-D-glucose and β-D-xylose degradation mechanisms in acidic aqueous solution. *Carbohydr. Res.* **2005**, *340*, 2319−2327.

(17) Xiang, Q.; Lee, Y. Y.; Torget, R. W. Kinetics of glucose decomposition during dilute-acid hydrolysis of lignocellulosic biomass. *Appl. Biochem. Biotechnol.* **2004**, *113*, 1127−1138.

(18) Li, J.; Henriksson, G.; Gellerstedt, G. Lignin depolymerization/repolymerization and its critical role for delignification of aspen wood by steam explosion. *Bioresour. Technol.* **2007**, *98*, 3061−3068.

(19) Mao, J.-D.; Holtman, K. M.; Scott, J. T.; Kadla, J. F.; Schmidt-Rohr, K. Differences between lignin in unprocessed wood, milled wood, mutant wood, and extracted lignin detected by ^{13}C solid-state NMR. *J. Agric. Food Chem.* **2006**, *54*, 9677−9686.

(20) Mao, J. D.; Cory, R. M.; McKnight, D. M.; Schmidt-Rohr, K. Characterization of a nitrogen-rich fulvic acid and its precursor algae from solid state NMR. *Org. Geochem.* **2007**, *38*, 1277−1292.

(21) Mao, J. D.; Tremblay, L.; Gagne, J. P.; Kohl, S.; Rice, J.; Schmidt-Rohr, K. Humic acids from particulate organic matter in the Saguenay Fjord and the St. Lawrence Estuary investigated by advanced solid-state NMR. *Geochim. Cosmochim. Acta* **2007**, *71*, 5483−5499.

(22) Selig, M.; Weiss, N.; Ji, Y. Enzymatic Saccharification of Lignocellulosic Biomass. *NREL/TP-510-42629*. National Renewable Energy Laboratory: Golden, CO, USA, 2008.

(23) Vlasenko, E. Y.; Ding, H.; Labavitch, J. M.; Shoemaker, S. P. Enzymatic hydrolysis of pretreated rice straw. *Bioresour. Technol.* **1997**, *59*, 109−119.

(24) Dence, C. W. The Determination of Lignin. In *Methods in Lignin Chemistry*; Dence, C. W., Lin, S. Y., Eds.; Springer-Verlag: Heidelberg, 1992; pp 33−61.

(25) Sluiter, A.; Hames, B.; Ruiz, R.; Scarlata, C.; Sluiter, J.; Templeton, D. Determination of Sugars, Byproducts, and Degradation Products in Liquid Fraction Process Samples. *NREL/TP-510-42623*. National Renewable Energy Laboratory: Golden, CO, USA, 2006.

(26) Blumenkrantz, N.; Asboe-Hansen, G. New method for quantitative determination of uronic acids. *Anal. Biochem.* **1973**, *54*, 484−489.

(27) Ralph, J.; Grabber, J. H.; Hatfield, R. D. Lignin-ferulate cross-links in grasses - active incorporation of ferulate polysaccharide esters into ryegrass lignins. *Carbohydr. Res.* **1995**, *275*, 167−178.

(28) Balakshin, M. Y.; Capanema, E. A.; Chen, C. L.; Gracz, H. S. Elucidation of the structures of residual and dissolved pine kraft lignins using an HMQC NMR technique. *J. Agric. Food Chem.* **2003**, *51*, 6116−6127.

(29) Mao, J. D.; Schmidt-Rohr, K. Separation of aromatic-carbon C-13 NMR signals from di-oxygenated alkyl bands by a chemical-shift-anisotropy filter. *Solid State Nucl. Magn. Reson.* **2004**, *26*, 36−45.
(30) Dixon, W. T. Spinning-sideband-free and spinning-sideband-only NMR-spectra in spinning samples. *J. Chem. Phys.* **1982**, *77*, 1800−1809.
(31) DeAzevedo, E. R.; Hu, W.-G.; Bonagamba, T. J.; Schmidt-Rohr, K. Principles of centerband-only detection of exchange in solid-state nuclear magnetic resonance, and extension to four-time centerband-only detection of exchange. *J. Chem. Phys.* **2000**, *112*, 8988−9001.
(32) Mao, J.-D.; Hundal, L. S.; Schmidt-Rohr, K.; Thompson, M. L. Nuclear magnetic resonance and diffuse-reflectance infrared fourier transform spectroscopy of biosolids-derived biocolloidal organic matter. *Environ. Sci. Technol.* **2003**, *37*, 1751−1757.
(33) Mao, J.-D.; Schmidt-Rohr, K. Absence of mobile carbohydrate domains in dry humic substances proven by NMR, and implications for organic-contaminant sorption models. *Environ. Sci. Technol.* **2006**, *40*, 1751−1756.
(34) Mao, J. D.; Xing, B. S.; Schmidt-Rohr, K. New structural information on a humic acid from two-dimensional H-1-C-13 correlation solid-state nuclear magnetic resonance. *Environ. Sci. Technol.* **2001**, *35*, 1928−1934.
(35) Mosier, N.; Wyman, C.; Dale, B.; Elander, R.; Lee, Y. Y.; Holtzapple, M.; Ladisch, M. Features of promising technologies for pretreatment of lignocellulosic biomass. *Bioresour. Technol.* **2005**, *96*, 673−686.
(36) Mao, J.-D.; Hu, W.-G.; Ding, G.; Schmidt-Rohr, K.; Davies, G.; Ghabbour, E. A.; Xing, B. Suitability of different ^{13}C solid-state NMR techniques in the characterization of humic acids. *Int. J. Environ. Anal. Chem.* **2002**, *82*, 183−196.
(37) Herzfeld, J.; Berger, A. E. Sideband intensities in NMR-spectra of samples spinning at the magic angle. *J. Chem. Phys.* **1980**, *73*, 6021−6030.
(38) Feather, M. S. The conversion of D-xylose and D-glucuronic acid to 2-furaldehyde. *Tetrahedron Lett.* **1970**, *48*, 4143−4145.
(39) Feather, M. S.; Harris, D. W.; Nichols, S. B. Routes of conversion of D-xylose, hexuronic acids, and L-ascorbic acid to 2-furaldehyde. *J. Org. Chem.* **1972**, *37*, 1606−1608.
(40) Harris, D. W.; Feather, M. S. Evidence for a C-2 → C-1 intramolecular hydrogen-transfer during the acid-catalyzed isomerization of D-glucose to D-fructose. *Carbohydr. Res.* **1973**, *30*, 359−365.
(41) Antal, M. J., Jr.; Leesomboon, T.; Mok, W. S.-L.; Richard, G. N. Mechanism of formation of 2-furaldehyde from D-xylose. *Carbohydr. Res.* **1991**, *217*, 71−85.
(42) McDonough, T. J. The chemistry of organosolv delignification. *TAPPI J.* **1993**, *76*, 186−193.
(43) Martínez, A. T.; Almendros, G.; González-Vila, F. J.; Fründ, R. Solid-state spectroscopic analysis of lignins from several Austral hardwoods. *Solid State Nucl. Magn. Reson.* **1999**, *15*, 41−48.
(44) Gil, A. M.; Neto, C. P. Solid-state NMR studies of wood and other lignocellulosic materials. *Annu. Rep. NMR Spectrosc.* **1999**, *37*, 75−117.
(45) Holtman, K. M.; Chen, N.; Chappell, M. A.; Kadla, J. F.; Xu, L.; Mao, J.-D. Chemical structure and heterogeneity differences of two lignins from loblolly pine as investigated by advanced solid-state NMR spectroscopy. *J. Agric. Food Chem.* **2010**, *58*, 9882−9892.

Received for review June 29, 2010. Revised manuscript received September 30, 2010. Accepted October 6, 2010. Partial support by the National Science Foundation (EAR-0843996 and CBET-0853950) is acknowledged.